Colloids and Surfaces A: Physicochemical and Engineering Aspects 655 (2022) 130246

Contents lists available at ScienceDirect

Colloids and Surfaces A: Physicochemical and Engineering Aspects

journal homepage: www.elsevier.com/locate/colsurfa

Yield stress of foam flow in porous media: The effect of bubble trapping

Haosen Zhang [a,b], Pablo R. Brito-Parada [b], Stephen J. Neethling [b], Yanghua Wang [a,b,*]

[a] Resource Geophysics Academy, Imperial College London, South Kensington, London SW7 2AZ, UK
[b] Department of Earth Science and Engineering, Imperial College London, South Kensington, London SW7 2AZ, UK

GRAPHICAL ABSTRACT

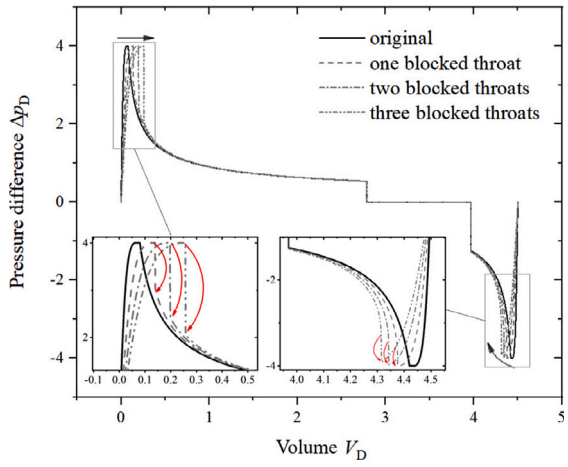

ARTICLE INFO

Keywords:
Foam
Porous media
Minimal surfaces
Bubble trapping
Yield stress

ABSTRACT

Foam behaves as a yield-stress fluid as it flows in a porous medium. Quasi-static analysis suggests that the yield stress arises from the non-smooth motion of foam films, denoted as lamellae, in pores. In order to study the effect of trapped lamellae on the motion of a moving lamella and consequently on the yield stress of foam, we conduct numerical simulations in the quasi-static limit. We propose a new method utilizing the surface energy minimization algorithm, which explicitly considers the connectivity of pores in a porous medium. We consider two different shapes of pore and vary the number of nearby trapped lamellae to investigate the effects of bubble trapping on the non-smooth and the smooth motion of a single lamella passing through a pore, respectively. We find that the trapped lamellae lead to the increased volume-averaged pressure drop and thus the increased yield stress. Notably, the motion of a lamella through a pore with rounded corners in the pore body becomes non-smooth, due to the presence of trapped lamellae. The results contribute to a better understanding of the yield stress of foam in porous media.

1. Introduction

Aqueous foam has found wide applications in industrial processes such as soil remediation [1,2], acid diversion in well stimulation [3], and EOR projects [4], for its ability to reduce gas mobility. In all these circumstances, foam is confined in porous media composed of a large number of irregular and varying-size pores contained in the solid matrix. Foam bubbles are thought to be of the same size or larger than the pores [5]. This is because newly generated bubbles by the snap-off,

* Corresponding author.
E-mail address: yanghua.wang@imperial.ac.uk (Y. Wang).

https://doi.org/10.1016/j.colsurfa.2022.130246
Received 9 May 2022; Received in revised form 20 September 2022; Accepted 25 September 2022
Available online 29 September 2022

which is a main foam generation mechanism in steady foam flow in porous media, are unlikely to be smaller than a pore body [6], and the gas diffusion driven by the pressure difference among bubbles tends to eliminate bubbles smaller than a pore [7–9]. Moreover, a significant amount of gas in a foam exists in the form of trapped bubbles [10]. In contrast, moving bubbles account for only a small fraction of gas. These moving bubbles form "bubble trains", which connect in sequence along the flow paths and squeeze through midst the trapped bubbles.

Rossen [11] studied the motion of a moving lamella in a pore which has two throats along the central axis of the pore and two side throats that are occupied by two trapped lamellae, respectively. A lamella enters the pore through one throat on the axis and moves forward to the opposite throat. As the lamella approaches the side throat, it will directly interact with the trapped lamellae. The results show that the motion of the moving lamella is complicated in the presence of trapped lamellae, compared to that of a lamella moving in a pore without side throats. In this paper, the effect of bubble trapping on the motion of moving bubbles is further investigated by considering that trapped lamellae are located in throats of other pores and indirectly interact with the moving lamella. For simplicity, we consider that lamellae propagate in a porous medium model which consists of several connected pores, and the gas in the foam is assumed to be incompressible. A two-level method, which minimizes the total surface energy of the foam system at two levels, i.e. at the sub-pore level and at the pore-network level, is proposed to calculate the foam configuration. This method is able to improve the computational efficiency, especially when the considered porous medium model is large. Another advantage is that the gas flow through pore throats can be tracked directly because the gas flow into each pore body is the variable solved in the simulations.

1.1. Background

Foam in porous media usually behaves as a yield-stress and shear-thinning fluid. Specifically, there exists a threshold of pressure gradient to start the foam flow, and the apparent viscosity of foam decreases as the flow velocity increases [12]. This minimum pressure gradient required to initiate foam flow arises from the resistance to deformation of thin foam films denoted as lamellae. The deformation of lamellae is in fact a complex interfacial phenomenon incorporating various dynamic processes as suggested in the work by Saye and Sethian [13] who proposed a multiscale modelling method to evolve the configuration of foam in bulk, though not in porous media. In their approach, gas dynamics in bubbles, liquid drainage within Plateau borders and foam lamellae, and lamella rupture are separated, given the fact of these processes' distinct characteristic time scales. These separated processes are handled separately and coupled in sequence to dynamically evolve the foam configuration.

In the limit of zero velocity, the movement of foam is quasi-static and its structure is of the minimum total surface energy, subjecting to constraints of finite and conserved bubble volumes as well as confined pore geometries [12,14]. One further simplification is the dry foam assumption, which is reasonable for a high-quality foam namely a foam with a low liquid fraction. The lamellae in a dry foam are represented as curved surfaces in 3D or curves in 2D, which are assumed to be stable, though a realistic foam could become increasingly unstable and probably destroyed by the film coalescence induced by the capillary suction as the foam quality increases [15]. Rossen [16] considered a 2D dry foam transport in a series of connected bi-conical pores and calculated the population-average pressure drop across the foam lamellae. It is suggested that a foam lamella would experience asymmetric pressure drop with respect to the volume swept by the lamella, which results in a net positive population-average pressure drop. This asymmetry arises from the asymmetric movement of the lamella front-to-back, because the lamella would spend more time moving in the diverging section of the pore than in the converging section of the pore, though the pore itself is symmetric front-to-back. A jump of the pressure difference happens when the lamella first enters the converging section of the pore, accompanied by the jump of the positions of the two wall Plateau borders. Moreover, the positions of the two wall Plateau borders after the jump could be symmetric or asymmetric about the central axis of the pore. Both the symmetric and asymmetric jumps of the wall Plateau borders have been discussed in the literature, which have distinct impact on the yield stress of foam [14,16]. The asymmetric jump of the two wall Plateau borders could lead to higher resistance and thus higher yield stress. Xu and Rossen [17] further considered the effect of viscous forces acting on the wall Plateau borders and proposed a dynamic model for the movement of lamella in 2D bi-conical pores. They suggested that as the velocity increases, the asymmetric jump happening as a lamella flows through the widest pore body is replaced by the symmetric jump.

The topology of foam structure is one important factor that affects the foam behaviour. The foam topology can be altered when bubbles are newly generated or destroyed. There are mainly three foam generation mechanisms in porous media, including leave-behind, snap-off and lamella division [18]. In the leave-behind mechanism, liquid films or lenses are left in the common throat of two adjacent pores as gas invades the pore bodies, which only applies in the initial drainage process. New bubbles can also be generated by snap-off when sufficient liquid accumulates near the geometric constrictions, i.e. pore throats, due to the capillary pressure fluctuation redistributing the liquid phase in porous media [19]. Incorporating the snap-off in simulations of foam flow would require additional modelling of the liquid phase within the foam lamellae in bulk as well as the wetting films coating on the walls. In contrast, lamella division is relatively easy to model as it simply divides a "mother lamella" into several new "daughter lamellae" whose number depends on the number of branch points that the "mother lamella" could hit. Cox [20] predicted the foam texture variation by implementing quasi-static simulations of a 2D dry foam in a straight channel containing a fixed disc. The foam texture is altered as the lamellae divide into new more lamellae when hitting the disc. It is shown that the foam topology can be further altered by a topological transformation named T1 transformation. The T1 transformation swaps the neighbouring bubbles associated with a lamella whose length shrinks to zero, which leads to the arising of an unstable four-fold connection point (in 2D) [21–24]. The T1 transformation mechanism does not change the number of bubbles, but it does alter the topology of foam configuration, and thus influences the following foam behaviour.

The pore connectivity of a porous medium also contributes to the complexity of foam behaviour. As a consequence of the pore connectivity, multiple flow paths co-exist in a porous medium. The active flow paths and hence the moving bubbles can be trapped when the flow resistance becomes sufficiently high [25]. In contrast, trapped bubbles can convert to flowing bubbles when the driving force is able to overcome the capillary resistance [25]. This flow pattern, i.e. flow intermittency, has enabled foam flooding with a sharp front in porous media because the trapped bubbles would block the previous preferential flow paths and activate new flow paths which would be blocked again as foam invades the porous media along the existing flow paths [26]. Jones et al. [27] experimentally studied the mobility of a dry foam in a simple model consisting of two parallel channels, and observed flow intermittency when a so-called bamboo-structure foam appears in one channel that is sufficiently narrow. This flow intermittency occurs because the spanning lamellae in the channel would be periodically pinned and then leave the exit of the channel into the downstream wide region. The flow rate decreased when a lamella was pinned due to the increased capillary pressure across the pinned lamella. This phenomenon suggests that foam behaviour in different flow paths are coupled, highlighting the importance of pore connectivity.

Previous studies have shed important insights into understanding the physical properties of foam flow in porous media. Foam structure

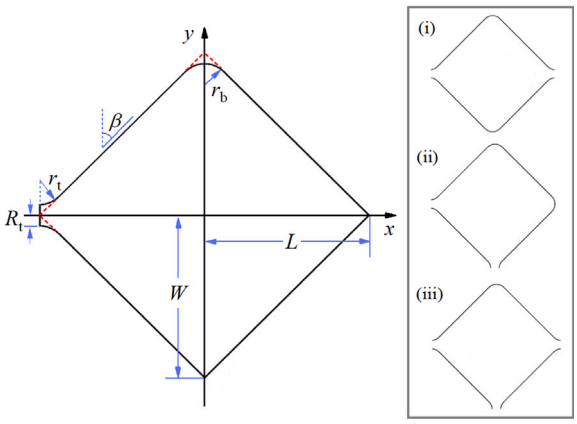

Fig. 1. Pore geometries used in this study are modified from a diamond. Geometric parameters are: L the half of pore length, W the half of pore width, R_t the half width of pore throat, r_b the rounding radius at corners in the pore body, r_t the rounding radius at the pore throats, and β the angle between the straight wall and the vertical. These parameters are not independent, i.e. $\beta = \tan^{-1}(W/L)$ and $R_t = (\sqrt{2}-1)r_t$. The pores used in this work include: (i) a pore with two opposite pore throats, (ii) a pore with two neighbouring pore throats, and (iii) a pore with three pore throats.

and capillary pressure can be locally tracked in theoretical and numerical studies, and foam morphology can be observed in micromodel experiments. However, the porous medium models used in previous theoretical and numerical studies have been relatively simple in how they represent a real porous medium, while the micromodel experiments failed to measure local physical quantities, such as the pressure in bubbles. To this end, we resort to quasi-static numerical simulations to further understand foam behaviour in a porous medium when connected flow paths are present.

2. Geometric models

The porous medium models used in this work are 2D models. To construct a porous medium, one straightforward way is to replace each site in a lattice pore network model with a pore possessing a specified shape. A reasonable size of such a pore network has been suggested by simulations of percolation behaviour performed on lattices [28]. Chatzis and Dullien [28] computationally simulated percolation behaviour in 2D lattice, arguing that a lattice width of 30 bonds and a length of 40 bonds is sufficient to reflect an infinite 2D lattices. For simplicity, we instead consider smaller geometric models. As shown later, even in such simpler models, the trapped lamellae exert significant influences on the movement of a lamella moving through a pore.

Several different geometric models are used in the present work, which are all constructed based on the individual pores depicted in Fig. 1. The pore shapes are derived from a diamond. To obtain the pores, the corners of the diamond are modified so that each corner represents a pore throat or a pore corner in the wide pore body. A pore corner is obtained by rounding a diamond corner with a selected radius. A small rounding radius results in a sharp pore corner. We consider two types of pore in the simulations, including the two-throat pore and the three-throat pore.

Table 1 presents the values taken for the related geometric parameters, which are dimensionless in this work. The radius at the corner in the central pore body is set to 0.25 and 1.0 for rounded and sharp pores, respectively. Both the pore length and width, i.e. $2L$ and $2W$, are set to 3.0. The typical dimensional length of a realistic pore might be 10 μm [26]. The corners are rounded because of the fact that pore corners could always be rounding due to the small amount of water occupying the corners, which can be brought by the Plateau borders moving along the walls [29,30]. We consider two different values of radius at the corners in the pore body, i.e. r_b equals 0.25 or 1.0. In addition, three

Table 1
Pore dimensions used in the simulations.

Geometric parameter (Dimensionless)	Value
L	1.5
W	1.5
R_t	0.207
r_b	0.25 and 1.0
r_t	0.25
β	$\pi/4$

types of pores are used, which are differentiated by the number of throats and the relative position of these throats, namely the two-throat pore with opposite throats, the two-throat pore with neighbouring throats and the three-throat pore. A two-throat pore with opposite throats is exactly a bi-conical pore as used in previous work [14,16,17]. A two-throat pore, either with opposite or neighbouring throats, is regarded as a sharp pore if r_b is set to 0.25, or a rounded pore if r_b is set to 1.0.

The geometric models used in this work are summarized in Fig. 2. In Section 4.1, we used the two-throat pore, shown in Fig. 2(i), to verify our code conducting the sub-pore level method discussed in Section 3.1. In the same subsection, we also constructed a porous medium composed of three pores, including one upstream three-throat pore and two downstream two-throat pores with neighbouring throats, in order to verify the pore-network method proposed in Section 3.2, as shown in Fig. 2(ii). We found that only one lamella would move forwards in the downstream pore with the remaining lamellae trapped in the pore throats, which is discussed in detail in Section 4.1. In Section 4.2, we considered the porous medium models shown in Fig. 2(iii)–(vi). The number of pores with trapped lamellae varies from 0 to 3, and for each case we considered that the pore with a moving lamella is sharp and rounded, respectively.

3. Method

To determine the foam configuration in equilibrium, the gradient descent method is used to evolve the foam system until the minimum surface energy is approached. The idea of the gradient descent method constructs the basis of the Surface Evolver [31], a computer software being able to computationally determine the foam configuration and the pressure drop across lamellae. In Surface Evolve, the foam configuration is evolved by moving the points on lamellae and, therefore, the foam configuration is predicted in a direct way. Since the geometric structures of the pore walls and the foam lamellae in the pores are directly modelled, we call the method used in the Surface Evolver the sub-pore level method. In the present work, we apply the idea at a different level, i.e. the pore-network level, where the foam movement is indirectly represented by the gas flow through pore throats. To differentiate this method from the sub-pore level method, we name this method the pore-network method. Here, we present both methods in detail, for comparison and completeness.

3.1. Sub-pore level

At this level, foam lamellae are discretized into material points whose positions determine the foam configuration, as embedded in the Surface Evolver [31]. Therefore, the evolution of the foam system is achieved by evolving the positions of these material points with calculated displacements by the gradient descent method. Discretization of foam lamellae and categories of associated geometric elements are shown in Fig. 3. In order to explain the sub-pore level method that can be used in a general circumstance of foam flow in 2D constricted pores, the schematic includes all the possible geometric elements, though some of these elements are not involved in the applications in the present work.

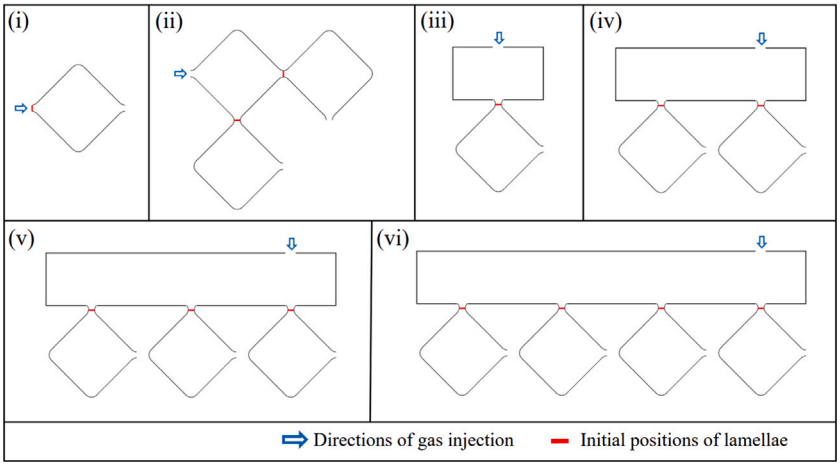

Fig. 2. Geometric models used in this work. (i) A single two-throat pore with opposite throats. (ii) A porous medium composed of three pores. (iii)–(vi) Porous medium models with the number of downstream pores varying from 1 to 4. The blue arrows show the direction that gas is injected into the models, and the red line segments show the initial positions of lamellae in the models. The models in (i) and (ii) are used in Section 4.1. The models in (iii)–(vi) are used in Section 4.2.

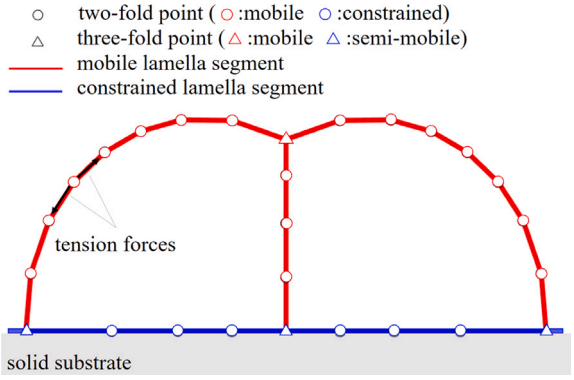

Fig. 3. Schematic of a foam configuration including two attached bubbles on the wall. Discretized segments of lamella in bulk include mobile lamella segments and constrained lamella segments. The constrained lamella is exactly the wetting film coating on the wall. The material points can be categorized into two-fold points and three-fold points, depending on the number of lamella segments that are connected through the points. A two-fold point can either be mobile or constrained. A mobile two-fold point is located on a mobile lamella, and a constrained two-fold point is attached on the wall. A three-fold point can either be mobile or semi-mobile. In physical terms, a mobile three-fold point is a bulk Plateau border, and a semi-mobile three-fold point is a wall Plateau border. This schematic is only referenced in the discussion of the sub-pore level method and may not accurately represent the realistic configuration.

We adopt linear interpolation to approximate the curved foam lamellae, i.e. the lamella segment between two neighbouring material points being represented by a straight line segment connecting the points. According to the number of edges that connect to a point, material points can be categorized into two-fold points and three-fold points. A two-fold point is an interior point on a lamella, while a three-fold point is the junction of three foam lamellae, i.e. the Plateau border. A Plateau border can be further specified as a bulk Plateau border or a wall Plateau border, depending on the Plateau border being in the bulk or on the wall.

Besides, according to the mobility of a point, material points can be categorized into four types namely fixed points, mobile points, semi-mobile points and constrained points. A material point is fixed when it is pinned on the wall. This is the case when a material point enters a wall section of high curvature, because the point is confined within that narrow region and hard to move. A mobile point is a two-fold point located interior of a lamella, with both connecting edges belonging to a mobile lamella that is in the pore space instead of coating on the wall. A semi-mobile point is a three-fold point located on the wall but is connected by a free lamella. A constrained point is a two-fold point on the constrained lamella coating on the wall.

3.1.1. Tension force of lamella

The surface in a foam system tends to minimize its total area because of the surface tension. The total tension force, F_i, acting on material point i is

$$F_i = \sum_{k=1}^{K} f_k, \tag{1}$$

where K, either 2 or 3, is the number of edges connecting to point i, and f_k is the tension force exerted by the kth connecting edge, which is a unit vector along the edge, pointing out of point i, as shown in Fig. 3. The tension forces acting on all the material points comprise the steepest descent direction of total surface energy for moving the material points [31]. Note that, only mobile lamellae would exactly exert a force on a material point. All the constrained lamellae coating on the walls, which are required to form enclosed bubbles, exert no force on any associated material points. This resultant evolving direction at each material point, however, needs to be modified, given the constraints that the bubble volume should be conserved and the semi-mobile points should always move tangentially along the wall.

The wall constraint requires that the tension force acting on a semi-mobile point should be projected to the tangent direction along the wall at that point, which can be separately calculated for each material point. In contrast, the bubble volume constraint results in a system of equations to be solved to determine the modification of tension force acting on each material point, because the bubble volume is expressed theoretically as an integral over all the material points on the boundary of a bubble. One way to calculate the modification is to utilize the gradient directions at each material point due to all the bubble volumes. Specifically, denote g_{ij} the gradient direction at point i due to the volume conservation in bubble j, which has been firstly projected onto the tangential plane of the wall. The modification of tension force at each point can be constructed as a linear combination of the gradient directions of all bubble volumes at that point [31]. Therefore, the modified evolution direction, F_i^v, at each point, is

$$F_i^v = F_i^p + \sum_{j=1}^{J} P_j g_{ij}^p, \tag{2}$$

where J is the number of bubbles, F_i^p the projected tension force, P_j the coefficient corresponding to the contribution of the jth bubble, and g_{ij}^p the direction projected from the gradient direction that the jth bubble exerts at the ith point.

The rate of the variation in volume of each bubble should be diminished if material points move along the directions given in Eq. (2), which leads to a linear system of equations for the unknown coefficients P_j

$$\sum_{i=1}^{N} F_i^v g_{ij}^p = 0, \quad j = 1, 2, \ldots, J, \tag{3}$$

where N is the number of material points of jth bubble. Solving this linear system of equations, the evolving direction of each material point can be determined. Furthermore, the displacement of each material point can be calculated as λF_i^v, where λ is a small scaling factor. Using a small scaling factor is important because the obtained directions evolving the positions of the material points only approximate the descent direction of the total surface energy to the first order. A small scaling factor ensures that the total surface energy is reduced after the foam configuration being evolved by the calculated displacement.

The evolution of the foam configuration is conducted using the iteration method. At each iteration step, the material points are moved by the calculated displacements. One problem remained, however, is the deviation in bubble volume after moving the foam configuration by the calculated displacements. Even though a small λ is used, which is helpful to maintain the bubble volume, the numerical error in the bubble volume could accumulate after a large number of iterations. The arising of this error can be explained from two aspects. Firstly, the modifications for the evolving directions are based on the bubble volumes' gradient directions at each material point. A finite displacement of a material point would lead to a second-order error in the bubble volume. Secondly, the number of material points discretizing the lamellae is finite in simulations. This discretization error could also lead to the deviation in bubble volume. In order to diminish the deviations in bubble volumes, volume restoring motion should be incorporated at each iteration step, immediately after the foam configuration being moved by the calculated displacements.

3.1.2. Volume restoring motion

The volume restoring motion, F_i^r, for each material point i, is expressed as a linear combination of the gradient direction of each bubble volume at the material point

$$F_i^r = \sum_{j=1}^{J} C_j g_{ij}^p, \tag{4}$$

where C_j is the coefficient corresponding to the contribution of the jth bubble. The volume restoring motions of all the material points would restore the volume for each bubble j, which is expressed as

$$\sum_{i=1}^{N} \left(\sum_{j'=1}^{J} C_{j'} g_{ij'}^p \right) g_{ij}^p = V_j^{\text{target}} - V_j, \tag{5}$$

where V_j is the current volume of bubble j, and V_j^{target} is the volume required to be restored. Eq. (5) can be written in a more convenient form shown in Eq. (6)

$$\sum_{j'=1}^{J} C_{j'} \left(\sum_{i=1}^{N} g_{ij'}^p g_{ij}^p \right) = V_j^{\text{target}} - V_j. \tag{6}$$

3.2. Pore-network level

The comparable bubble size with respect to the pore size, in the context of EOR, has inspired the idea that apply the gradient descent method at the pore-network level. A pore throat is less likely to be occupied by multiple foam lamellae as the case of a bulk foam in a container, meaning that uniform pressure distributes in the pore throat. The presence of foam lamellae in a pore body would lead to pressure differences among pore throats connecting to the pore body.

We divide a large porous medium into individual pores connected by pore throats, as shown in Fig. 4. Different colours are used to differentiate a pore from its adjacent pores. The scheme of the division is not unique and could be altered during a simulation process because some throats could be sufficiently wide to allow simultaneous passage of multiple lamellae. For the pore marked in pink in the central area of the porous medium shown in Fig. 4, we notice that the variation in the total surface energy of the lamellae in the pore, which in the sub-pore level method is related to the displacements of the material points on the lamellae, could be re-expressed using two physical quantities, i.e. the pressure differences among the throats of the pore and the gas flow through these throats.

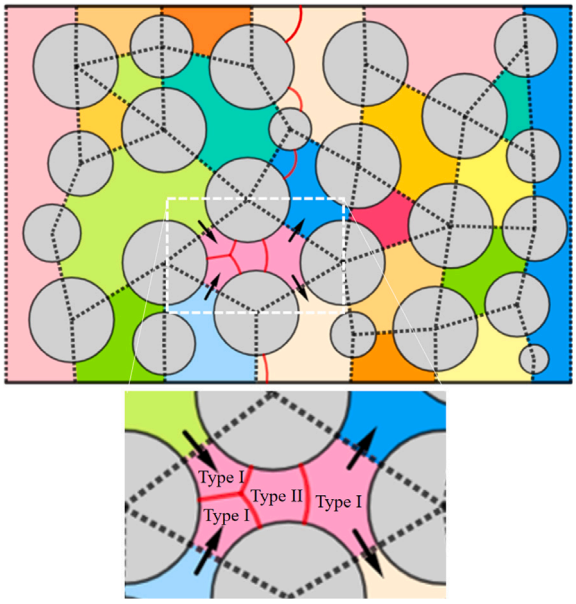

Fig. 4. Schematic of a 2D porous medium. The circles in grey are solid grains and the void space is divided into pores connected by pore throats. Pores are marked in different colours. The red curves are the assumed configuration of foam lamellae in the porous medium. The black arrows illustrate the assumed directions of gas flowing through the pore throats that surround the pore in pink at the centre of the porous medium. Differentiating the gas area or bubble of type I from type II, Type I refers to the gas area being enclosed by pore throats, pore wall and lamellae, and type II is the bubble enclosed by pore wall and lamellae. The idea of the pore-network level method is to express the variation in the total surface energy in the pore as a form in terms of the pressure differences among the pore throats and the gas flow though these pore throats.

3.2.1. Mass conservation in pores

Gas is conserved in any pore in the porous medium. Denote f_{pt} the gas flow through pore throat t of pore p. In default, f_{pt} is positive when gas flows into pore p and negative when gas leaves the pore. The mass conservation in pore p is

$$\sum_{t=1}^{T} f_{pt} = 0, \tag{7}$$

where T is the number of throats of pore p. Therefore, the gas flow through a specific throat of a pore can be represented using the gas flow through all other throats of that pore. For instance, gas flow through pore throat $t = 1$ is written as

$$f_{p1} = -\sum_{t=2}^{T} f_{pt}. \tag{8}$$

3.2.2. Gradient of system energy

There are two types of gas areas (or called bubbles) as shown in Fig. 4, categorized upon the boundaries that enclose the gas areas. Specifically, type I refers to the bubble that is enclosed by pore throats, pore wall and lamellae, and type II is the bubble enclosed by pore

wall and lamellae, namely individual bubbles that do not span several pores. We denote the volume of gas area of type I as V_{pt}, where p is the identification of the pore and t is the identification of the throat belonging to that pore. Denoting the pressure at pore throat t of pore p as P_{pt}, the pressure potential energy of the gas in the pore, E_p, can be expressed as

$$E_p = \sum_{t=1}^{T} P_{pt} V_{pt} + \text{Const}, \tag{9}$$

where V_{pt} is the volume of the bubble of type I attached to pore throat t. The term, Const, accounts for the energy in bubbles of type II. Note that it is possible that a type I bubble is bounded by two or more throats. In this case, the gas potential energy in that bubble would be counted repeatedly in Eq. (9). This repetition does not affect the energy variation because the pressure at these throats associated with this type I bubble is the same, and thus the pressure difference among these throats is zero.

Considering infinitesimal gas perturbation, f_{pt}, the first-order approximation of the variation in the pressure potential energy in pore p is

$$\delta E_p = \sum_{t=1}^{T} P_{pt} f_{pt}, \tag{10}$$

where f_{pt} is considered as an infinitesimal gas flow through pore throat t. This energy variation is exactly the net work done in pore p and is stored as film surface energy. Substituting Eq. (8) into Eq. (10), the energy variation becomes

$$\delta E_p = 0 \cdot f_{p1} + \sum_{t=2}^{T} (P_{pt} - P_{p1}) f_{pt}, \tag{11}$$

where the first term on the right hand side, with coefficient 0, is added for completeness.

The variation of the total surface energy, δE, in the whole porous medium, can be obtained by summarizing the energy variation over all the pores in the porous medium

$$\delta E = \sum_{p=1}^{Z} 0 \cdot f_{p1} + \sum_{p=1}^{Z} \sum_{t=2}^{T} (P_{pt} - P_{p1}) f_{pt}, \tag{12}$$

where Z is the number of pores in the porous medium.

For a given porous medium, Eq. (12) can be further simplified into a form that the total energy variation is expressed as a linear function of the gas flow through pore throats.

$$\delta E = \sum_{t=1}^{Y} g_t(\Delta P) f_t, \tag{13}$$

where Y is the number of all the pore throats in the porous medium and g_t the coefficient of gas flow, which is a function of pressure difference appearing in Eq. (12), and f_t the absolute value of gas flow through pore throat t. Note that the subscript t now is a global index denoting one specific pore throat in the porous medium, instead of the local index denoting throats of an individual pore.

To exemplify the transformation from Eq. (12) to Eq. (13), we consider the porous medium model shown in Fig. 2(ii), which is studied in Section 4.1. The scheme to divide the porous medium model is shown in Fig. 5. For this model, the specific expression of Eq. (12) can be written as

$$\begin{aligned}\delta E =& 0 \cdot f_{11} + (P_{12} - P_{11}) f_{12} + (P_{13} - P_{11}) f_{13} + \\ & 0 \cdot f_{21} + (P_{22} - P_{21}) f_{22} + \\ & 0 \cdot f_{31} + (P_{32} - P_{31}) f_{32},\end{aligned} \tag{14}$$

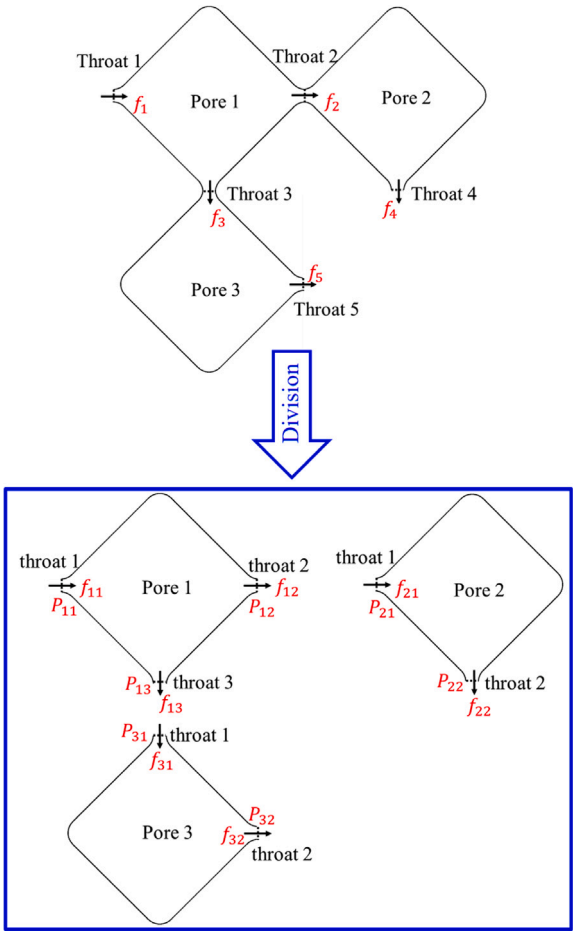

Fig. 5. The division scheme for the three-pore porous medium model considered in Section 4.1. The model is divided into three connected pores, including a three-throat pore and two two-throat pores, whose indices p are 1, 2, 3, respectively. There are 5 throats in this model, whose global indices t are 1, 2 ..., 5. The assumed directions of the gas flow are shown by the black arrows. f_t is the absolute value of the gas flow through throat t of the porous medium model. P_{pt} is the pressure at the throat of local index t of pore p. f_{pt} is the gas flow through the throat t of pore p, which is either positive or negative, depending on the gas flow is into or out of pore p. When referring to a specific pore, the local index t of a throat of the pore is up to 2 or 3.

which can be further combined into a form as in Eq. (13). It is known that

$$\begin{aligned} &f_1 = f_{11}, \\ &f_2 = -f_{12}, f_2 = f_{21}, \\ &f_3 = -f_{13}, f_3 = f_{31}, \\ &f_4 = -f_{22}, \\ &f_5 = -f_{32}. \end{aligned} \tag{15}$$

Substituting Eq. (15) into Eq. (14), we obtain

$$\delta E = 0 \cdot f_1 - (P_{12} - P_{11}) f_2 - (P_{13} - P_{11}) f_3 - (P_{22} - P_{21}) f_4 - (P_{32} - P_{31}) f_5, \tag{16}$$

where the coefficients of f_t are denoted as $g_t(\Delta P)$ in Eq. (13). These coefficients namely pressure differences among pore throats can be obtained using the sub-pore level method or, in simple cases, by the analytical solution.

Eq. (13) shows that the gas flow through each pore throat is $f_t = -g_t(\Delta P)$, and enables us to evolve the foam system by the gas flow through pore throats. The remaining issue is that the gradient descent direction $-g_t(\Delta P)$, which only provides guessed values of gas flow

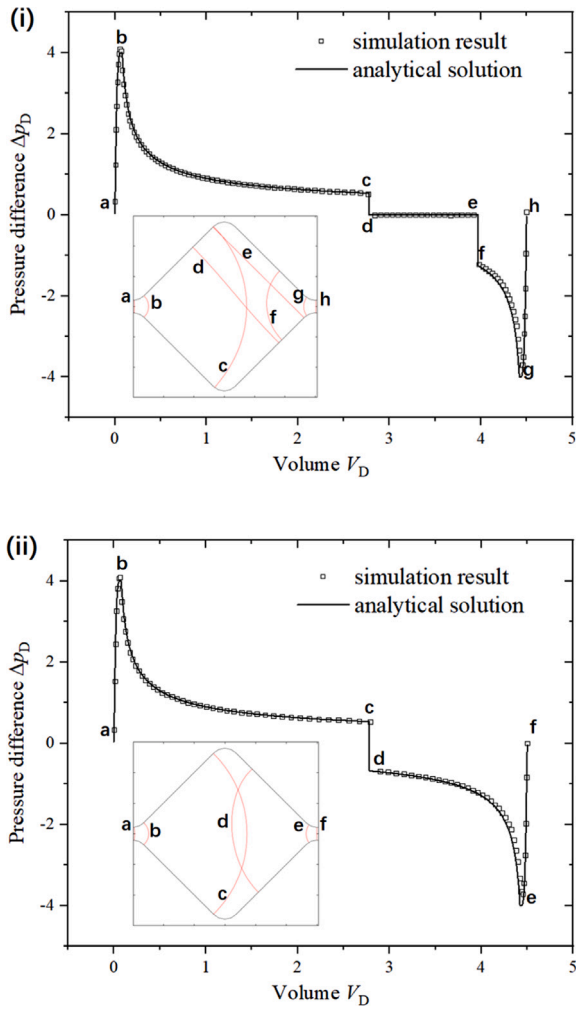

Fig. 6. Processes of a lamella passing through a pore with two opposite throats are simulated. The results of the pressure drop across the lamella are compared with the analytical solution. The letters refer to the lamella shapes in the inserted figures. (i) Asymmetric jump. Two Plateau borders become asymmetric about the horizontal axis of the pore after approaching the corners in the wide pore body (ii) Symmetric jump. During the lamella propagation, two Plateau borders maintain symmetric about the horizontal axis of the pore. The analytical solution for the symmetric and asymmetric jump is available in [16].

through each pore throat, could disobey the mass conservation law, and should be modified. To do so, we write Eq. (7) in a form with respect to the absolute value of the gas flow through pore throats as

$$\sum_{t=1}^{Y} k_{pt} f_t = 0, \tag{17}$$

where k_{pt} is a coefficient, taking 0, 1, or −1. The coefficient occurs because f_t has been taken as the absolute value of gas flow through pore throat t and its direction is ruled in advance for a specific porous medium, as exemplified in Eq. (15).

The modification for each gradient component given by Eq. (13) is assumed to be $-\sum_{p=1}^{Z} K_p k_{pt}$ with K_p being the coefficient associated with the mass conservation in pore p. Thus, f_t is modified as $-g_t(\Delta P) - \sum_{p=1}^{Z} K_p k_{pt}$. To solve the unknown coefficients, the modified gas flow through each pore throat should satisfy the total Z mass conservation equations. We substitute $f_t = -g_t(\Delta P) - \sum_{p=1}^{Z} K_p k_{pt}$ into Eq. (17) and obtain

$$\sum_{t=1}^{Y} k_{pt} \left(g_t + \sum_{p=1}^{Z} K_p k_{pt} \right) = 0, \tag{18}$$

which can be transferred into a convenient form

$$\sum_{p=1}^{Z} K_p \sum_{t=1}^{Y} k_{pt} = -\sum_{t=1}^{Y} k_{pt} g_t. \tag{19}$$

Eq. (19) is a counterpart of Eq. (6) derived for the sub-pore level. An addition equation to be solved together with Eq. (19) is that the amount of gas injected in a porous medium model is known. For instance, in the previous example using the porous medium model in Fig. 5(ii), f_1 equals δV which is a small increment of gas volume assigned in simulations.

Finally, the resultant gas flow through each pore throat can be written as $f_t = -\lambda\left(g_t + \sum_{p=1}^{Z} K_p k_{pt}\right)$, where λ is a small scaling factor. The scaling factor is needed because the total surface energy is non-linearly varied with the gas flow through each pore throat. The surface energy reduction is guaranteed only when the adjustment to the foam configuration is minor.

3.3. Algorithm

There are at least two distinct algorithms, based on the methods discussed in Sections 3.1 and 3.2, for conducting quasi-static simulations for foam flow in a porous medium. The simplest and most straightforward way is to apply the sub-pore level method in a confined geometry, e.g. a porous medium, without dividing a porous medium into smaller parts, as has been conducted in many studies [14,20,32–34]. Another algorithm (hereafter we call it the two-level method) relies on both the sub-pore and the pore-network level methods, which is most efficient when gas bubbles are, in general, larger than the size of pores because we have based the pore-level method on uniform pressure distribution in pore throats recognized as the most restricted area in the local geometry.

In the two-level method, after a small amount of gas, δV, is injected into the geometric model, the sub-pore level and the pore-network level methods are implemented alternatively and a sufficient number of iterations are needed to obtain the convergent foam configuration. For each iteration step, after the gas flow through each pore throat has been determined using the pore-network level method and is injected into each pore, the sub-pore level method is applied to calculate the pressure distribution in each pore. Then the pressure differences among pore throats can be calculated and serve as the input for the pore-network level method in the next iteration. Note that, in order to simulate the injection of gas, the total gas flow through the pore throats connected to the injection port is set to δV in the first iteration. In the remaining iterations leading to the convergent foam configuration, this total gas flow is set to 0.

4. Numerical results

4.1. Verification of the method

The code implementing the sub-pore level method is verified by simulating a single lamella moving through a single pore with two opposite throats. The simulation results of the pressure drop across the lamella, denoted as Δp_D, which is varied with the volume swept by the lamella since its entering the pore, denoted as V_D, are in good agreement with the analytical solution, as shown in Fig. 6. We reproduce both the asymmetric and the symmetric jump of the two wall Plateau borders when the lamella propagates through the central pore body. In numerical simulations, the symmetric jump occurs when a relatively large volume increment is applied to push the lamella forward in the pore [14]. In physical terms, as the lamella approaches the corners with a large velocity, the perturbations, which lead to an asymmetric lamella shape, are still small when the lamella has arrived in the converging pore section on both sides, and thus a symmetric jump occurs [17]. For realistic movements in the quasi-static limit, the asymmetric jump shown in Fig. 6(i) will always occur, with the symmetric behaviour

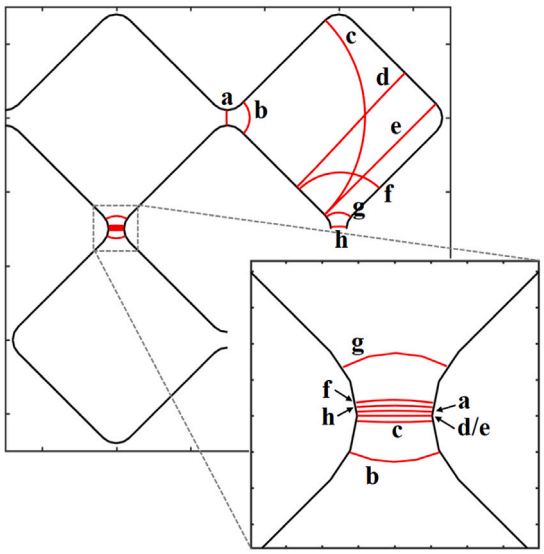

Fig. 7. The geometry used to verify the two-level method consists of a three-throat pore and two two-throat pores. Lamella configurations are labelled by letters ordered in the alphabetic sequence. Initially, two lamellae are positioned right in the two interior pore throats. Though the shapes of the two downstream pores are the same and the initial lamella configuration is symmetric, the movements of the two lamellae are asymmetric, with one lamella trapped nearby the pore throat and the other propagating through the downstream pore.

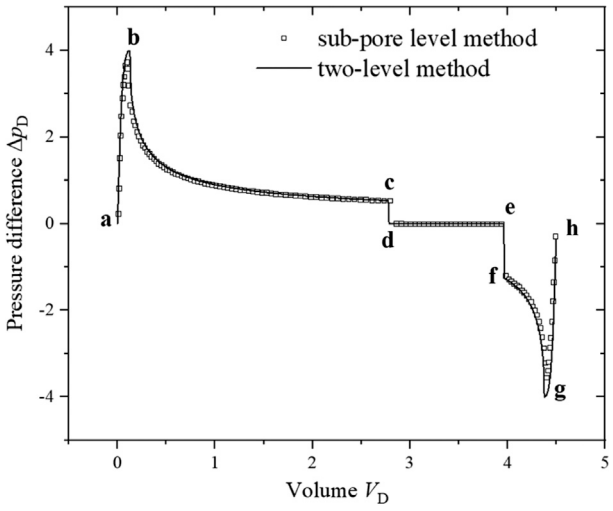

Fig. 8. The pressure difference across the three-pore model calculated by the sub-pore level method and the two-level method. For lamella positions and shapes labelled by the letters, one refer to Fig. 7.

shown in Fig. 6(ii) being shown purely to demonstrate the significant impact that the asymmetry has on the pressure profile as the lamella traverses the pore. At high gas rates where viscous drag is appreciable the asymmetric jump may be suppressed, though this case is not considered in this work. For further discussion of the effects of the jump, one can refer to [14,32].

To verify the idea using the gradient descent method at the pore-network level, we consider a geometry composed of two pores with two neighbouring throats and one three-throat pore, as shown in Figs. 2(ii) and 5. Initially, both interior pore throats, i.e. "Throat 2" and "Throat 3" in Fig. 5, are blocked by a lamella, and these two lamellae are flat with zero pressure drop across them. Foam configuration at the initial moment is denoted by the letter, a. Then gas is injected into the geometric model through the top-left pore throat and allowed to leave the model through the two pore throats connected to the external space, i.e. "Throat 4" and "Throat 5" in Fig. 5. The injection of gas continues until one lamella approaches either one of the two outlets. The pressure drop across the geometric model and the gas flow through the two interior pore throats are predicted by the sub-pore level method and the two-level method, respectively, and compared in Figs. 8 and 9.

The results of the two-level method are in agreement with those of the sub-pore level method, suggesting the validity of the two-level method. It is shown that the pressure difference across the model experiences an asymmetric jump due to the asymmetric movements of the Plateau borders. Moreover, bubble trapping occurs in one of the pore throats as the gas mainly flows through the other pore throat. Although the two downstream pores are symmetrically positioned in the porous medium model, the symmetric displacement of the two lamellae in the two downstream pores is less likely to happen as this motion mode is unstable, which would transfer to the stable mode namely the asymmetric displacement pattern under small perturbations.

The sub-pore level method always results in the stable displacement pattern due to the discretization error of the foam system, which acts to disturb the positions of the two lamellae in the two downstream pores. Using the two-level method, the unstable displacement mode can be reproduced, but this motion mode is broken if small perturbations in the gas flow through pore throats are introduced in the iterations. In other words, the stable motion mode requires only one moving lamella with all other lamellae trapped nearby the pore throats, which applies when there are multiple downstream pores in the porous medium model as discussed later in Section 4.2.

Note that, in the two-level method, sub-pore level simulations are usually needed because the related pressure differences are required as the input in the pore-network level simulations. For simple foam configurations, the pressure differences among throats can also be obtained by the analytical solution. In this study, we use the analytical solution of the pressure drop across the pore with two neighbouring throats as the input in the implementation of the two-level method.

4.2. Investigation on the effect of bubble trapping

In this subsection, we use the geometric model, shown in Fig. 2(iii)–(vi), to further investigate the motion of a moving lamella in the presence of trapped lamellae. The number of downstream pores varies from 1 to 4. As all the throat geometries connecting the upstream pore and the downstream pores are the same, the stable motion mode, as suggested in last subsection, would be that only one lamella moves through the downstream pore while all other lamellae are trapped in the pore throats. As a consequence, the number of trapped lamellae varies from 0 to 3. When there is only one downstream pore, the problem reduces to that a single lamella moves through a single pore with two neighbouring throats. We denote the result of this case as "original". As defined in Section 2, the downstream pore that a lamella moves through is considered as a sharp or rounded pore when the rounding radius, r_b, at the central pore body is 1.0 or 0.25. We firstly consider the case that the downstream pore is sharp namely $r_b = 1.0$.

4.2.1. Lamella moving in the sharp downstream pore

The pressure difference across the geometric model with sharp downstream pores is shown in Fig. 10, from which mainly three distinct phenomena can be observed. Firstly, both the positive and the negative peaks of the pressure difference are displaced towards the mid point of the horizontal axis, compared to the case that the upstream pore has only one downstream pore with two neighbouring throats, i.e. the "original" case. Specifically, the positive peak is delayed because a small amount of gas flows through the trapped pore throat and is stored in that region, as illustrated by configurations a to b in Fig. 7 and the gas flow through each pore throat in Fig. 9(ii). In the opposite, the negative peak occurs earlier than expected because the previously

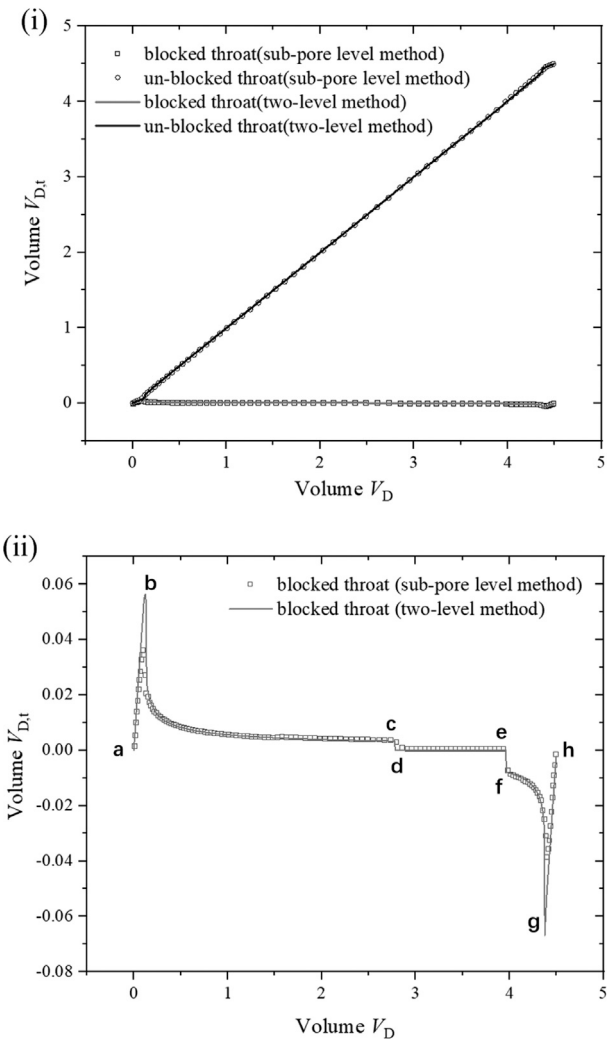

Fig. 9. The gas flow from the upstream pore to the two downstream pores through two interior throats, varied with the total amount of gas injected into the three-pore porous medium model. (i) The amount of gas flowing through two throats, denoted as $V_{D,t}$, calculated by the sub-pore level method and the two-level method, are in agreement. The magnitude contrast in terms of the gas amount through the two throats shows that the gas mainly flows through one pore throat while the other pore throat is blocked by the lamella. (ii) The gas flow through the blocked throat is separately plotted to show more details with respect to the variation in gas amount through the blocked throat versus the total gas amount injected into the three-pore porous medium model. For lamella positions and shapes labelled by the letters, one refer to Fig. 7.

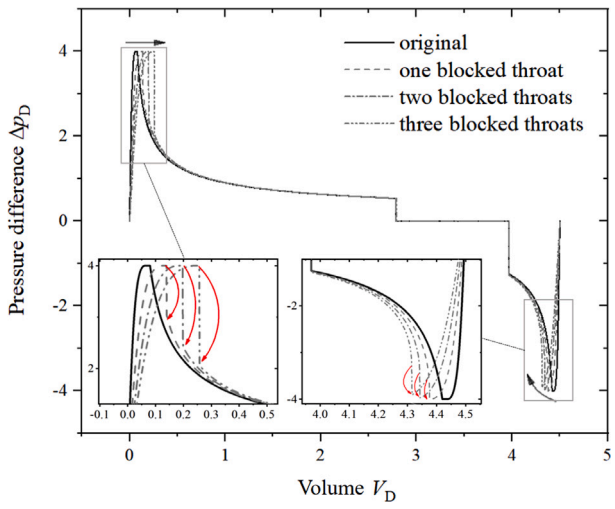

Fig. 10. The pressure difference versus the gas amount injected into the geometric model with the sharp downstream pore, i.e. r_b equals 0.25, is influenced by the trapped lamellae. In addition to the jump of the pressure difference that happens as a lamella moves through the central pore body, the jump also occurs when the positive peak is left or the negative peak is approached, as denoted by the red arrows in the insert figures. Trends of the variations in the positions and the magnitudes of the peaks are marked by the black arrows. The positive peak is delayed while its magnitude maintains. In contrast, the negative peak happens earlier than expected and its magnitude declines if more lamellae are trapped.

stored gas in the trapped throat has been released in the later period when the lamella moves through the second-half section of the pore.

Secondly, a jump of the pressure difference happens immediately after the positive peak or before the negative peak, and the jump is enlarged if more throats are trapped by lamellae. Lastly, the magnitude of the negative peak decreases as the number of trapped lamellae increases. The positive peaks, instead, maintain the same magnitude, not influenced by the presence of trapped lamellae.

In the original case, there is no trapped lamellae and thus the overall symmetry of the variation in pressure difference ΔP_D with the injected gas volume V_D is only broken by the jump of wall Plateau borders happening in the central region of the pore body. The two peak regions remain central symmetric about the midpoint on the horizontal axis. In the presence of trapped lamellae, the three phenomena, especially the last two phenomena, deteriorate the symmetry of the variation in the pressure difference. Specifically, the symmetry of the two peak regions is further broken because the magnitudes of the two peaks are no longer the same and the jumps at both peaks are not symmetric. In addition, a superposition effect is observed that this symmetry breaking is enhanced as more lamellae are trapped in the throats.

In order to explain the arising of the above phenomena and their effects, we consider the case shown in Fig. 1(vi) and keep in mind that the stable motion mode is that only one lamella moves through the pore while all other lamellae are trapped. We utilize the variation of pressure difference as a function of gas volume for a single lamella moving through a single pore and that for three lamellae trapped in the pore throats. For the latter, the maximum total amount of gas volume injected into the three downstream pores is up to 0.177. Moreover, we extended the curve into negative domain of the horizontal axis because the three trapped lamellae become convex toward the upstream pore when the pressure difference across the moving lamella becomes negative. Setting the pressure difference as the control variable and considering the pressure difference independent of flow paths, an interpolation curve can be obtained from the curves of the pressure difference varied with the gas volume for a moving lamella and three trapped lamellae, respectively, as shown in Fig. 11. This interpolated curve shows that the amount of gas injected into the porous medium model varies non-monotonically if the pressure difference is continuously varied, which conflicts with the fact that the injection of gas into the model is continuous. As a consequence, a jump of pressure difference is invoked to maintain the increasing injection of gas, as shown in the "modification" curve in Fig. 11, which further changes the magnitude of the negative peak.

In addition to the three phenomena discussed above, the middle jump of the pressure difference is only slightly delayed in the presence of trapped lamellae, compared to the "original" case, and thus only slightly deteriorates the symmetry of the variation of the pressure difference versus the volume of gas injected into the model. The most significant effects that the trapped lamellae exert on the motion of a single lamella remain to be the three phenomena discussed above. As discussed later, these phenomena could also happen when the moving lamella is in a rounded pore whose r_b equals 1.0.

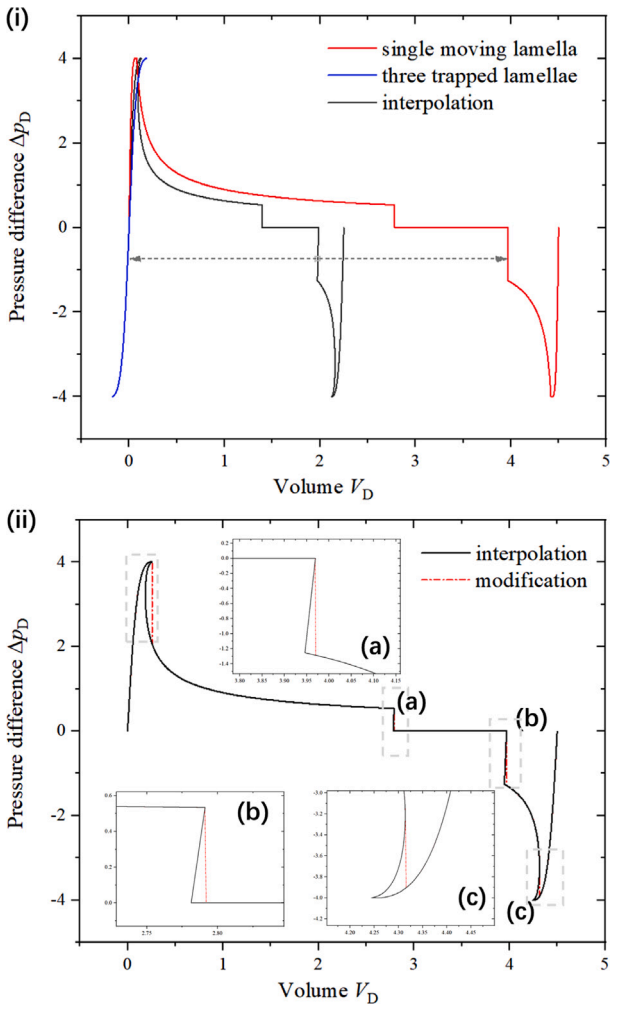

Fig. 11. The pressure difference across the porous medium model shown in Fig. 1(vi) as a function of gas volume injected into the model. (i) The total volume of gas injected into the porous medium model equals the sum of the gas volume flowing into all downstream pores. The pressure difference varied with injected gas volume (the red solid curve) for a single lamella moving through a single pore and that for three lamellae trapped in throats (the blue solid curve) are used for the interpolation. The grey dashed line segment and its midpoint illustrate the interpolation by taking the average of the gas volumes at two curves given the same value of the pressure difference. Thus, the "interpolation" curve has its horizontal coordinate representing the half of the amount of gas injected into the porous medium model. (ii) The interpolated solid curve in (i) is doubled in terms of the horizontal coordinate and then is modified to meet the requirement of continuous gas injection. The modifications at the two peaks are not symmetric. Specifically, the magnitude of the positive peak maintains while the magnitude of the negative peak declines.

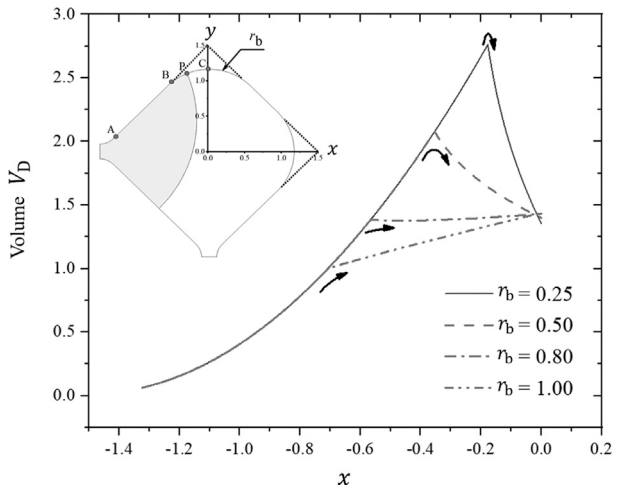

Fig. 12. The variation in bubble volume swept by a lamella versus the horizontal coordinate of the Plateau border contacting on the upper wall of the pore. The swept bubble volume is marked by the area in grey in the insert figure. The sharpness of the corner is controlled by the rounding radius, r_b. For sharp corners, e.g. r_b equals 0.25 or 0.50, the volume decreases after the upper Plateau border enters the corner. To avoid a decrease in volume, the lamella would generally jump to a new position, which results in the jump of the pressure difference. For rounded corners, e.g. r_b equals 0.80 or 1.00, the volume continuously increases as the upper Plateau border moves along the upper pore wall.

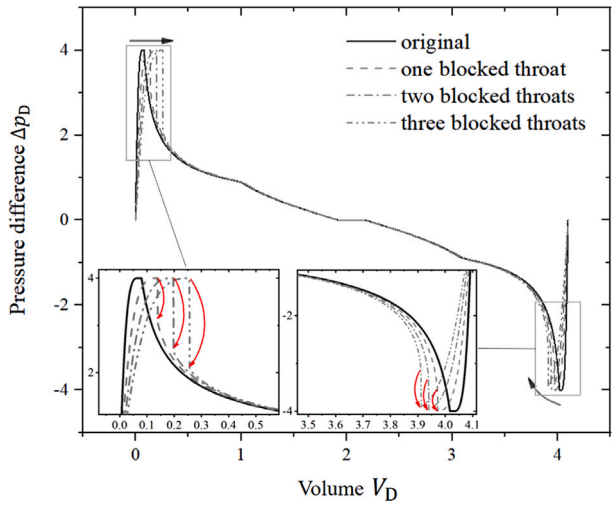

Fig. 13. The pressure difference across the geometric model with the downstream pore being rounded, i.e r_b equals 1.0. The pressure difference is influenced by the trapped lamellae. No jump occurs as the moving lamella passes through the central pore body. However, a jump occurs at both peaks, as denoted by the red arrows in the inset figures. Trends of the variations in the positions and the magnitudes of the peaks are marked by the black arrows. The positive peak is delayed while its magnitude maintains the same. In contrast, the negative peak occurs earlier than expected and its magnitude declines as more lamellae are trapped.

4.2.2. Lamella moving in the rounded downstream pore

Simulation results of a single lamella propagating through a single bi-conical pore suggest that a rounded pore, i.e. a pore with a large rounding radius at its corners in the central pore body, is differentiated from pores with sharp corners, in terms of the average flow resistance [14,32]. A lamella flowing in a rounded pore would have its average flow resistance being zero. In Fig. 12, the insert schematic shows a lamella in a pore with two neighbouring throats, whose configuration meets the rule of a 90-degree contact angle between the pore walls and the lamella. It shows that the volume swept by the lamella may not increase continuously when the Plateau borders move continuously on the pore walls, depending on the sharpness of the corner in the pore body.

When the radius at the corner is small, e.g. r_b equals 0.25, the volume decreases as the wall Plateau borders moves along the curved corner. To maintain a continuous increase of the bubble volume, the wall Plateau borders have to jump to new positions, which further results in the jump of pressure difference. In contrast, for large radius at the corner, e.g. r_b equals 1.00, the continuous increase of bubble volume is guaranteed and no jump of the wall Plateau borders is expected.

The pressure difference versus the injected gas volume in the case of the rounded downstream pore, i.e. r_b equals 1.00, is shown by the "original" curve in Fig. 13. The variation is purely central symmetric around the midpoint on the horizontal axis, which means the average flow resistance would be zero. However, when trapped lamellae are

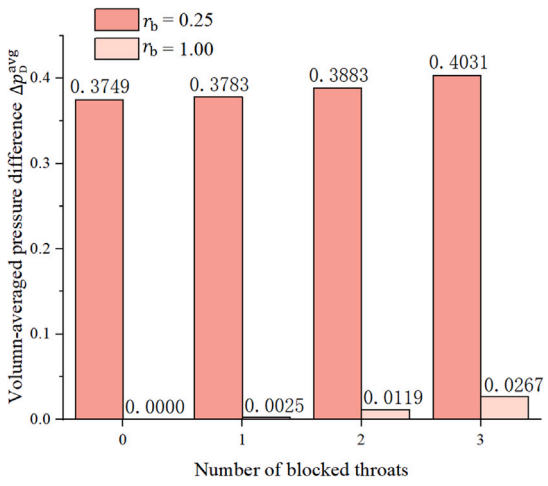

Fig. 14. Variation in the volume-averaged pressure difference for the porous medium models composed of pores with sharp corners, i.e. r_b equals 0.25, and rounded corners, i.e. r_b equals 1.00, respectively. For the same number of downstream pores, the increment of the volume-averaged pressure difference due to the presence of trapped lamellae is nearly the same for both cases. The influence of the trapped lamellae on the volume-averaged pressure difference could be significant when a large number of trapped lamellae are present. In relative terms, the trapped lamellae have a more apparent influence in the cases with rounded pores, leading to non-zero flow resistance. The absolute increasing in the volume-averaged pressure difference, however, is similar for the two different r_b values.

present, we observe the same effects of the trapped lamellae as those in Fig. 10, namely displaced positions of both positive and negative peaks, jumps of the pressure difference at peaks, and declined magnitude of the negative peak. As a consequence of these effects, the averaged flow resistance or the yield stress, which is represented as the volume-averaged pressure difference, becomes non-zero.

4.2.3. The volume-averaged pressure difference

The volume-averaged pressure difference is calculated as

$$\Delta p_D^{avg} = \frac{1}{V_{tot}} \int_0^{V_{tot}} \Delta p_D dV_D, \tag{20}$$

where Δp_D^{avg} is the volume-averaged pressure difference and V_{tot} is the total amount of gas injected into the medium. Fig. 14 shows the effects of trapped lamellae on the volume-averaged pressure difference in both cases of the sharp downstream pore and the rounded downstream pore.

We find that the trapped lamellae lead to the increase in the volume-averaged pressure difference of a single lamella moving through a pore, suggesting that the resistance of foam flow not only arises from the moving lamella but also from the trapped lamellae with limited mobility. This effect becomes stronger as more lamellae are present and trapped in the nearby pore throats. This is important especially for the cases with rounded pores because the flow resistance becomes non-zero, which means the decrease in the foam mobility.

5. Discussion

The non-smooth motion of lamellae in confined geometries leads to flow resistance even at an infinitesimal small flow rate. Simulation results show that the trapped lamellae not only block the associated flow paths, but also affect the motion of moving lamellae in other flowing paths, thus contributing to the yield stress of foam flow in confined geometries. The presence of trapped lamellae results in the arising of the non-zero yield stress even for those porous medium models composed of rounded pores. The mechanism of this effect is associated with the competition of pressure differences along different flow paths. The pressure differences are determined by the foam configuration and would vary as the foam propagates in a porous medium. Specifically, the gas volume injected into the model is not the same as the volumetric advance of the lamella, due to the presence of trapped lamellae with limited mobility. This effect is similar to the effect of gas compressibility depicted by Rossen [30] that the increasing pressure difference can delay the advance of the lamella and thus affects the yield stress of foam in porous media.

The mobility of lamellae, namely being either trapped or mobile, relies on the shapes of pores in a porous medium. For the quasi-static movement, the dominant factor is the maximum pressure difference across a lamella moving through a pore. For example, consider the three-pore porous medium model with two downstream pores of the same shape and name the two downstream pores A and B. If a lamella moves through either A or B, the maximum pressure difference is the same. This leads to three possible motion modes: (1) one lamella is trapped in the throat of A while the other lamella moves through B, (2) one lamella is trapped in the throat of B while the other lamella moves through A, and (3) both lamellae move through A and B. The pore-network level method shows that motion mode (3) is not stable because the total surface energy can be further reduced under perturbations of lamella positions. However, if pore A is slightly different from B and leads to a larger maximum pressure difference, the possible motion mode becomes unique, i.e. mode (1).

The cases considered in the present work involve several trapped lamellae but only one moving lamella. Therefore, our understanding of the yield stress of foam is limited to relatively simple flow cases happening at the pore scale [11,14,16,17,29,30,32,35]. Several aspects could be improved to release this limitation. Firstly, large porous medium models and concentrated distribution of foam lamellae are preferred in order to mimic a realistic case. Pores with large coordination numbers could facilitate more complicated lamella interactions because these pores function as the junctions of multiple “bubble trains”. The lamella interaction could also be enhanced as the foam becomes more fine-textured. Secondly, though simulations based on the dry foam assumption can incorporate some important phenomena such as gas diffusion [33] and bubble division [20], there are some other important effects that instead could not be easily incorporated. For instance, as an important lamella generation mechanism in porous media, the snap-off relies on the water accumulation near constricted pore throat regions and is suggested to be dependent on the capillary fluctuation in porous media [19,36]. Another example regarding the redistribution of the liquid phase is the capillary suction coalescence that could occur as a lamella stretches in the wide pore body, which has impact on the lamella stability [37]. Finally, dynamic foam behaviour cannot be reproduced under the quasi-static assumption, such as the process of the jump predicted in the quasi-static simulations and the process of topological transformation events that could happen in a foam flow process [22,38].

6. Conclusions

In this work, we conducted quasi-static simulations to further understand foam behaviour at the extreme of infinitesimal flow rate. Especially, we focus on the effects of bubble trapping on the yield stress of foam in porous media. We firstly proposed a two-level method being able to minimize the total surface energy at the pore-network level, which utilizes the connectivity of pores in a porous medium. In our simulation of the quasi-static behaviour of multiple lamellae in simple porous media, it was demonstrated that the only stable propagation mode was for a single lamella to move through the system, with the other lamellae remaining trapped in pore throats. Though these trapped lamellae do not interact with the moving lamella directly, the averaged flow resistance for the lamella moving through the downstream pore is enhanced as the number of trapped lamellae increases. This is because the trapped lamellae can affect the gas flow along different flow paths and adjust the pressure distribution in the porous medium.

In the future, it would be interesting to consider quasi-static foam flow in a large porous medium, incorporating more foam behaviour, such as bubble division and gas diffusion. In addition, the lamella mobility has been discussed under the quasi-static assumption. Beyond this assumption such as taking into account the viscous dissipation acting on the wall Plateau borders, there could exist multiple lamella moving along different flow paths in a porous medium, which would also be of interest to be considered.

CRediT authorship contribution statement

Haosen Zhang: Conceptualization, Methodology, Validation, Writing & editing. **Pablo R. Brito-Parada:** Conceptualization, Writing & editing. **Stephen J. Neethling:** Conceptualization, Writing & editing. **Yanghua Wang:** Conceptualization, Writing & editing.

Declaration of competing interest

The authors declare that they have no known competing financial interests or personal relationships that could have appeared to influence the work reported in this paper.

Data availability

No data was used for the research described in the article.

Acknowledgements

The authors are grateful to the sponsorship of the Resource Geophysics Academy, Imperial College London, for supporting this research.

References

[1] P. Chowdiah, B. Misra, J. Kilbane II, V. Srivastava, T. Hayes, Foam propagation through soils for enhanced in-situ remediation, J. Hard Mater. 62 (3) (1998) 265–280, http://dx.doi.org/10.1016/S0304-3894(98)00191-5.

[2] S. Wang, C. Mulligan, An evaluation of surfactant foam technology in remediation of contaminated soil, Chemosphere 57 (9) (2004) 1079–1089, http://dx.doi.org/10.1016/j.chemosphere.2004.08.019.

[3] L. Cheng, S. Kam, M. Delshad, W. Rossen, Simulation of dynamic foam-acid diversion processes, in: SPE European Formation Damage Conference, 2001, http://dx.doi.org/10.2118/68916-MS.

[4] R. Farajzadeh, A. Andrianov, H. Bruining, P. Zitha, Comparative study of CO2 and N2 foams in porous media at low and high pressure-temperatures, Ind. Eng. Chem. Res. 48 (9) (2009) 4542–4552, http://dx.doi.org/10.1021/ie801760u.

[5] R. Prud'homme, Foams: Theory, Measurements, and Applications, Routledge, New York, 2017.

[6] Q. Chen, M. Gerritsen, A. Kovscek, Modeling foam displacement with the local-equilibrium approximation: Theory and experimental verification, SPE J. 15 (01) (2010) 171–183, http://dx.doi.org/10.2118/116735-PA.

[7] A. Falls, J. Lawson, G. Hirasaki, The role of noncondensable gas in steam foams, J. Pet. Technol. 40 (01) (1988) 95–104, http://dx.doi.org/10.2118/15053-PA.

[8] W. Rossen, M. Wang, Modeling Foams for Acid Diversion. SPEJ 4 (2): 92–100, Tech. Rep., SPE-56396-PA, 1999, http://dx.doi.org/10.2118/56396-PA.

[9] S. Jones, N. Getrouw, S. Vincent-Bonnieu, Foam flow in a model porous medium: I. The effect of foam coarsening, Soft Matter 14 (18) (2018) 3490–3496, http://dx.doi.org/10.1039/C7SM01903C.

[10] S. Jones, N. Getrouw, S. Vincent-Bonnieu, Foam flow in a model porous medium: II. The effect of trapped gas, Soft Matter 14 (18) (2018) 3497–3503, http://dx.doi.org/10.1039/C7SM02458D.

[11] W. Rossen, Minimum pressure gradient for foam flow in porous media: Effect of interactions with stationary lamellae, J. Colloid Interface Sci. 139 (2) (1990) 457–468, http://dx.doi.org/10.1016/0021-9797(90)90118-8.

[12] A. Mauray, M. Chabert, H. Bodiguel, Yield stress fluid behavior of foam in porous media, Phys. Rev. Fluids 5 (9) (2020) 094004, http://dx.doi.org/10.1103/PhysRevFluids.5.094004.

[13] R. Saye, J. Sethian, Multiscale modeling of membrane rearrangement, drainage, and rupture in evolving foams, Science 340 (6133) (2013) 720–724, http://dx.doi.org/10.1126/science.1230623.

[14] S. Cox, S. Neethling, W. Rossen, W. Schleifenbaum, P. Schmidt-Wellenburg, J. Cilliers, A theory of the effective yield stress of foam in porous media: The motion of a soap film traversing a three-dimensional pore, Colloids Surf. A 245 (1–3) (2004) 143–151, http://dx.doi.org/10.1016/j.colsurfa.2004.07.004.

[15] K. Ma, J. Lopez-Salinas, M. Puerto, C. Miller, S. Biswal, G. Hirasaki, Estimation of parameters for the simulation of foam flow through porous media. Part 1: The dry-out effect, Energy Fuels 27 (5) (2013) 2363–2375, http://dx.doi.org/10.1021/ef302036s.

[16] W. Rossen, Theory of mobilization pressure gradient of flowing foams in porous media: I. Incompressible foam, J. Colloid Interface Sci. 136 (1) (1990) 1–16, http://dx.doi.org/10.1016/0021-9797(90)90074-X.

[17] Q. Xu, W. Rossen, Effective viscosity of foam in periodically constricted tubes, Colloids Surf. A 216 (1–3) (2003) 175–194, http://dx.doi.org/10.1016/S0927-7757(02)00547-2.

[18] H. Hematpur, S. Mahmood, N. Nasr, K. Elraies, Foam flow in porous media: Concepts, models and challenges, J. Nat. Gas Sci. Eng. 53 (2018) 163–180, http://dx.doi.org/10.1016/j.jngse.2018.02.017.

[19] W. Rossen, A critical review of roof snap-off as a mechanism of steady-state foam generation in homogeneous porous media, Colloids Surf. A 225 (1–3) (2003) 1–24, http://dx.doi.org/10.1016/S0927-7757(03)00309-1.

[20] S. Cox, Simulations of bubble division in the flow of a foam past an obstacle in a narrow channel, Colloids Surf. A 473 (2015) 104–108, http://dx.doi.org/10.1016/j.colsurfa.2014.10.038.

[21] D. Weaire, M. Fortes, Stress and strain in liquid and solid foams, Adv. Phys. 43 (6) (1994) 685–738, http://dx.doi.org/10.1080/00018739400101549.

[22] T. Green, A. Bramley, L. Lue, P. Grassia, Viscous froth lens, Phys. Rev. E 74 (5) (2006) 051403, http://dx.doi.org/10.1103/PhysRevE.74.051403.

[23] D. Reinelt, A. Kraynik, Simple shearing flow of dry soap foams with tetrahedrally close-packed structure, J. Rheol. 44 (3) (2000) 453–471, http://dx.doi.org/10.1122/1.551096.

[24] C. Torres-Ulloa, P. Grassia, Viscous froth model applied to the motion and topological transformations of two-dimensional bubbles in a channel: Three-bubble case, Proc. Royal Soc. A (2022) http://dx.doi.org/10.1098/rspa.2021.0642.

[25] Z. Pang, X. Lyu, F. Zhang, T. Wu, Z. Gao, Z. Geng, C. Luo, The macroscopic and microscopic analysis on the performance of steam foams during thermal recovery in heavy oil reservoirs, Fuel 233 (2018) 166–176, http://dx.doi.org/10.1016/j.fuel.2018.06.048.

[26] S. Xiao, Y. Zeng, E. Vavra, P. He, M. Puerto, G. Hirasaki, S. Biswal, Destabilization, propagation, and generation of surfactant-stabilized foam during crude oil displacement in heterogeneous model porous media, Langmuir 34 (3) (2018) 739–749, http://dx.doi.org/10.1021/acs.langmuir.7b02766.

[27] S. Jones, B. Dollet, Y. Méheust, S. Cox, I. Cantat, Structure-dependent mobility of a dry aqueous foam flowing along two parallel channels, Phys. Fluids 25 (6) (2013) 063101, http://dx.doi.org/10.1063/1.4811178.

[28] I. Chatzis, F. Dullien, Modelling pore structure by 2-D and 3-D networks with applicationto sandstones, J. Can. Pet. Technol. 16 (01) (1977) 97–108, http://dx.doi.org/10.2118/77-01-09.

[29] W. Rossen, Theories of foam mobilization pressure gradient, in: SPE Enhanced Oil Recovery Symposium, OnePetro, 1988, http://dx.doi.org/10.2118/17358-MS.

[30] W. Rossen, Theory of mobilization pressure gradient of flowing foams in porous media: III. Asymmetric lamella shapes, J. Colloid Interface Sci. 136 (1) (1990) 38–53, http://dx.doi.org/10.1016/0021-9797(90)90076-Z.

[31] K. Brakke, The surface evolver, Experiment. Math. 1 (2) (1992) 141–165, http://dx.doi.org/10.1080/10586458.1992.10504253.

[32] D. Ferguson, S. Cox, The motion of a foam lamella traversing an idealised bi-conical pore with a rounded central region, Colloids Surf. A 438 (2013) 56–62, http://dx.doi.org/10.1016/j.colsurfa.2013.02.015.

[33] L. Nonnekes, S. Cox, W. Rossen, Effect of gas diffusion on mobility of foam for enhanced oil recovery, Transp. Porous Media 106 (3) (2015) 669–689, http://dx.doi.org/10.1007/s11242-014-0419-z.

[34] S. Cox, I. Davies, Simulations of quasi-static foam flow through a diverging-converging channel, Korea-Aust. Rheol. J. 28 (3) (2016) 181–186, http://dx.doi.org/10.1007/s13367-016-0018-3.

[35] W. Rossen, Theory of mobilization pressure gradient of flowing foams in porous media: II. Effect of compressibility, J. Colloid Interface Sci. 136 (1) (1990) 17–37, http://dx.doi.org/10.1016/0021-9797(90)90075-Y.

[36] W. Rossen, Comment on "verification of roof snap-off as a foam-generation mechanism in porous media at steady state", Colloids Surf. A 322 (1–3) (2008) 261–269, http://dx.doi.org/10.1016/j.colsurfa.2008.02.034.

[37] A. Jimenez, C. Radke, Dynamic stability of a foam lamella flowing through a periodically constricted tube, Am. Chem. Soc., Div. Pet. Chem., Prepr.;(United States) 33 (CONF-880659) (1988) https://escholarship.org/uc/item/62k5h8v4.

[38] N. Kern, D. Weaire, A. Martin, S. Hutzler, S. Cox, Two-dimensional viscous froth model for foam dynamics, Phys. Rev. E 70 (4) (2004) 041411, http://dx.doi.org/10.1103/PhysRevE.70.041411.